Available online at www.sciencedirect.com
ScienceDirect
Biochimica et Biophysica Acta 1767 (2007) 653 – 659
Biochimica et Biophysica Acta
BBA
www.elsevier.com/locate/bbabio

Bio-photosensor: Cyanobacterial photosystem I coupled with transistor via molecular wire

Nao Terasaki [a], Noritaka Yamamoto [a], Kaoru Tamada [a], Mineyuki Hattori [a], Takashi Hiraga [a,*], Akihiko Tohri [b], Ikutaro Sato [b], Masako Iwai [b], Michinao Iwai [b], Shunpei Taguchi [b], Isao Enami [c], Yasunori Inoue [b,*], Yoshinori Yamanoi [d], Tetsu Yonezawa [d], Katsuya Mizuno [d], Masaki Murata [d], Hiroshi Nishihara [d,*], Satoshi Yoneyama [e], Makoto Minakata [e,*], Tsutomu Ohmori [f], Makoto Sakai [f], Masaaki Fujii [f,*]

[a] *Photonics Research Institute, National Institute of Advanced Industrial Science and Technology, 1-8-31 Midorigaoka, Ikeda, Osaka 563-8857, Japan*
[b] *Department of Applied Biological Science, Faculty of Science and Technology, Tokyo University of Science, Yamazaki 2641, Noda, Chiba 278-8510, Japan*
[c] *Department of Biology, Faculty of Science, Tokyo University of Science, 1-3 Kagurazaka, Shinjuku-ku, Tokyo 162-8601, Japan*
[d] *Department of Chemistry, School of Science, The University of Tokyo, 7-3-1 Hongo, Bunkyo-ku, Tokyo 113-0033, Japan*
[e] *Research Institute of Electronics, Shizuoka University, 3-5-1 Johoku, Hamamatsu, Shizuoka 432-8011, Japan*
[f] *Chemical Resources Laboratory, Tokyo Institute of Technology, 4259 Nagatsuta-cho, Midori-ku, Yokohama 226-8503, Japan*

Received 30 September 2006; revised 6 November 2006; accepted 9 November 2006

Abstract

We report on the first successful output of electrons directly from photosystem I (PSI) of thermophilic cyanobacteria to the gate of a field-effect transistor (FET) by bypassing electron flow via a newly designed molecular wire, i.e., artificial vitamin K_1, and a gold nanoparticle; in short, this newly manufactured photosensor employs a bio-functional unit as the core of the device. Photo-electrons generated by the irradiation of molecular complexes composed of reconstituted PSI on the gate were found to control the FET. This PSI-bio-photosensor can be used to interpret gradation in images. This PSI-FET system is moreover sufficiently stable for use exceeding a period of 1 year.

Keywords: Cyanobacterial photosystem I; Gold nanoparticle; Molecular wire; Field-effect transistor; Bio-photosensor

1. Introduction

Photosynthesis is among the most impressive phenomena on earth, not only because it has given rise to the world as we know it, but also because it has provided abundant inspiration for major scientific inquiry into clean and inexhaustible solar energy [1,2], water splitting [3,4], carbon dioxide and nitrogen fixation [5,6], and most importantly, the almost 100%-efficient photo-electric conversion systems involved in the primary process of photosynthesis [7,8]. This ultimate system developed over a period of the four billion years of the evolution cycle. Photosynthesis has fascinated a large number of scientists, who have expended much effort to imitate this process; however, the artificial induction of functional biosystems has been rare [9]. In spite of the difficulty of such an approach, the use of the photosynthetic protein complexes that regulate photosynthesis appears to be reasonable for the investigation of photosynthetic bio-systems.

A large number of trials have been conducted to date involving the application of such biological systems to

---

* Corresponding authors. T. Hiraga is to be contacted at fax: +81 72 751 9637. Y. Inoue, fax: +81 4 7123 9767. H. Nishihara, fax: +81 3 5841 8063. M. Minakata, fax: +81 53 478 1322. M. Fujii, fax: +81 45 924 5250.

E-mail addresses: hiraga-t@aist.go.jp (T. Hiraga), inoue_y@rs.noda.tus.ac.jp (Y. Inoue), nisihara@chem.s.u-tokyo.ac.jp (H. Nishihara), minakata@rie.shizuoka.ac.jp (M. Minakata), mfujii@res.titech.ac.jp (M. Fujii).

0005-2728/$ - see front matter © 2006 Elsevier B.V. All rights reserved.
doi:10.1016/j.bbabio.2006.11.008

electronic devices. For example, in a few studies, chloroplasts were spread on an SnO_2 electrode and were examined as photoelectrochemical cells [10,11]. Recently, the chloroplast has been investigated in terms of how the orientation of proteins strongly affects the transfer of bionic electrons to an electrode [12–14]. The high performance of PSI is the result of its well-designed spatial configuration (position, direction, etc.); however, no investigations using the PSI photonic device in this context have been reported to date. In this paper, we discuss the first successful direct coupling between functional bionic components (PSI) to artificial electronic devices (FET) via a molecular electric wire designed at the molecular order (Fig. 1); in addition, the output of electrons from PSI to FET is demonstrated with the aim of obtaining a PSI-bio-photosensor capable of interpreting the gradation in an image.

2. Materials and methods

2.1. Materials

Thermophilic cyanobacteria *Thermosynechococcus elongatus* strain BP1 was used as an origin of photosystem I complex (PSI). All chemical reagents were obtained from commercial sources and used without additional purification. FET chips (No. 001314) with an Si_3N_4–Ta_2O_5 thin layer-covered gate were purchased from BAS Inc.

2.2. Characterization

^{1}H NMR and ^{13}C NMR spectra were recorded on a Bruker DRX-500 instrument at room temperature. Chemical shifts in ppm were referenced to tetramethylsilane (0.00 ppm) as an internal standard. EI-MS measurements were recorded on a Shimadzu GCMS-QP5000A. FAB-MS spectra were recorded on a JMS SX-102 mass spectrometer (JEOL). Elemental analysis of the products was performed on a Yanaco MT-6 C, H, N corder at the Elemental Analysis Center of the University of Tokyo. Quartz crystal microbalance (QCM) measurements were carried out with a Hokuto HQ-101B QCM controller.

2.3. Isolation of PSI

The cultivation, isolation, and purification of PSI were carried out according to well-known procedures reported in the literature [15].

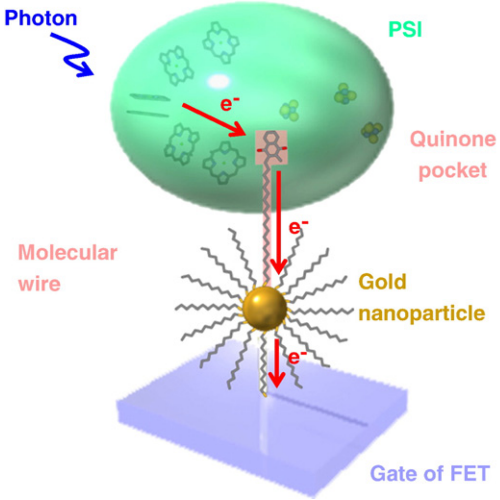

Fig. 1. The concept of the bio-photosensor made of PSI coupled with transistor via molecular wire.

2.4. Synthesis of molecular wire and surfactant

2-(15-Bromopentadecyl)-3-methyl-1,4-naphthoquinone, 1-[15-(3-methyl-1,4-naphtoquionon-2-yl)]pentadecyl disulfide (($NQC_{15}S)_2$), 1-[15-(3-methyl-1,4-naphtoquionon-2-yl)]pentadecyl thiolate-protected gold nanoparticles ($NQC_{15}S$-AuNP) [16], 1-bromo-12-phenoxydodecane, and (12-phenoxydodecyl)triethylammonium bromide were newly synthesized according to the procedures shown in Scheme 1. The details of the reaction conditions and characterization are described in Supplementary Information.

2.5. Reconstitution of PSI with molecular wires

Purified PSI samples were washed with pure water six times to remove the detergents from the surface of PSI. Next, samples were dried up by lyophilizer (Tokyo Rikakikai FD-1000) for 2 days. To remove VK_1 from PSI, the dry samples were suspended in 50% water-saturated diethyl ether (1 mg dried PSI / 5 mL diethyl ether) for 10 min at 4 °C, then diethyl ether was removed by centrifugation. This treatment was repeated twice. The VK_1-free PSI was re-suspended in 20 mM MES-buffer containing (12-phenoxydodecyl)triethylammonium bromide (PSI:(12-phenoxydodecyl)triethylammonium bromide = 1:300). To reconstitute PSI, $NQC_{15}S$-AuNP was added to the PSI solution (PSI:$NQC_{15}S$-AuNP = 1:1) and gently stirred for 1 day at 4 °C. Excess $NQC_{15}S$-AuNP was removed by five times ultrafiltration using centrifugal filter (Millipore Amicon ultrafree-MC 100,000NMWL) and pure reconstituted PSI, $NQC_{15}S$-AuNP@PSI, was obtained.

2.6. PSI photoactivity measurements

A modified double beam spectrophotometer (Hitachi Model 557) was used to determine the formation of cation of reaction center chlorophyll a in PSI ($P700^{+}$) under actinic blue light irradiation. Broad band actinic blue light (25 Wm^{-2}) was obtained by the combination of a 30 W tungsten lamp and 10 mm path 20% $CuSO_4$ water solution. PSI sample solution was contained in a disposable polystyrene cuvette having 10 mm measuring light (701 nm) path and 3 mm actinic blue light path. To eliminate contamination of actinic light to a photo-multiplier, an interference filter transmitted 701 nm light (Optical Coatings Japan) was put on the surface of photo-multiplier.

2.7. TEM measurements

The TEM images of the intact PSI and $NQC_{15}S$-AuNP@PSI were recorded at 75 kV using a Hitachi H-7000 system, and the $NQC_{15}S$-AuNP image was obtained at 200 kV using a Hitachi HF-2000 system. The solutions of native and modified PSI molecules were dropped on the carbon-coated copper grids. The samples were not subjected to staining.

2.8. Photocurrent measurements

A self-assembled monolayer (SAM) of 1,4-benzenedimethanethiol was prepared on the surface of the gold electrode by immersing an Au-mica plate which had been annealed by hydrogen frame just before use in an ethanol solution of 10 mM 1,4-benzenedimethanethiol. Then, $NQC_{15}S$-AuNP@PSI was immobilized on the SAM via Au-S bond by immersing the SAM-modified gold electrode in a buffer solution d containing the reconstituted PSI for 24 h.

Photocurrent measurements were carried out with the electrochemical cell equipped with an Ag/AgCl reference electrode and a Pt counter electrode in the presence of 250 mM sodium L-ascorbate (NaAs) as a sacrificial reagent, 2.5 mM 2,6-dichloroindophenol sodium hydrate (DCIP) as a mediator, and 100 mM $NaClO_4$ in the MES-NaOH (pH 6.4) buffer aqueous solution. The $NQC_{15}S$-AuNP@PSI-immobilized Au-mica electrode was irradiated with a monochromatic light from an Asahi Spectra LAX100 Xe lamp, passed through an optical filter (Asahi Spectra, $\Delta\lambda = \pm 6.5$ nm). The light intensity was 3.3 mW at 680 nm, and the irradiation area was 0.16 cm^2. With controlling the electrode potential by a FUSO HECS318C potentiostat, the current responses with the light irradiation were measured and recorded as the photocurrent.

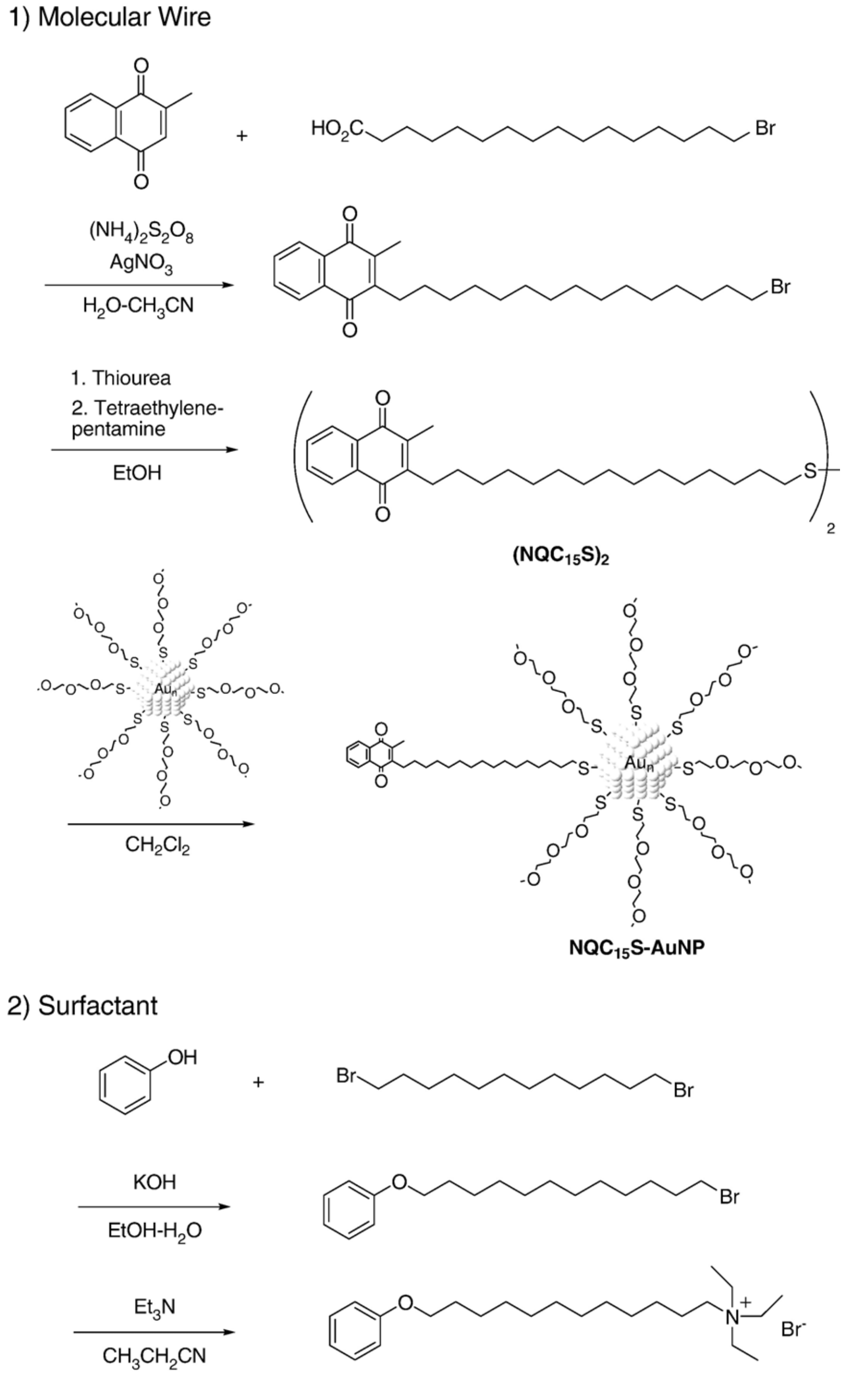

Scheme 1. Preparation procedures of molecular wire and surfactant.

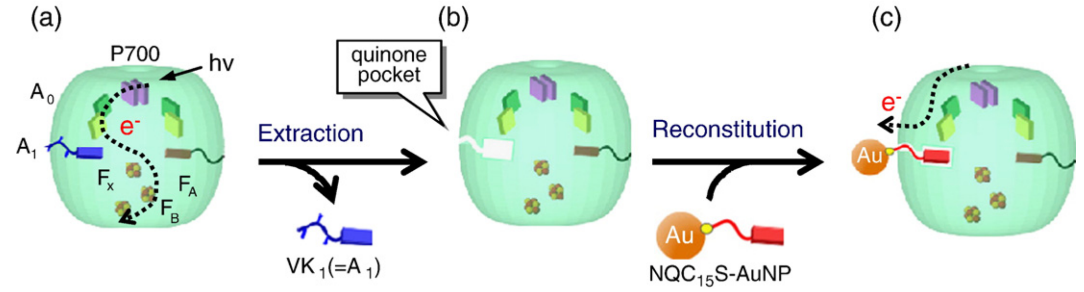

Fig. 2. Schematic illustration of the procedure for the reconstitution of PSI with a molecular wire: (a) intact PSI, (b) VK_1-free PSI, and (c) $NQC_{15}S$-AuNP@PSI.

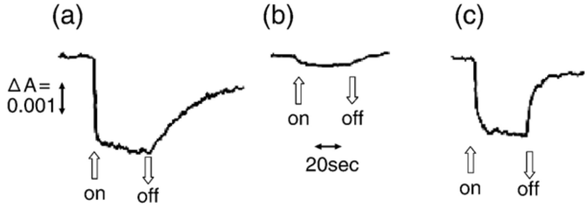

Fig. 3. Blue light induced absorption decrease at 701 nm for intact PSI (a), VK1-free PSI (b), and $NQC_{15}S$-AuNP@PSI (c). Upward arrow indicates the starting point of blue light irradiation, and downward arrow indicates the end point of blue light irradiation.

2.9. Fabrication and performance of the $NQC_{15}S$-AuNP@PSI-immobilized FET photosensor

An Si_3N_4–Ta_2O_5 thin layer on the gate of an FET was treated with an ethanol solution of 5% bis[3-(triethoxysilyl)propyl] tetrasulfide for 1 h at room temperature. Then, the FET gate was immersed in a buffer solution of $NQC_{15}S$-AuNP@PSI for 24 h. The photo-response of the FET was measured under the same conditions described in former section, and the results were recorded by a BAS 001400 mV/pH meter. The original equipment was slightly modified so as to readout a current below 1 μA. All measurements were carried out at room temperature. We fixed the voltage between the source and the drain (V_{SD}), and measured the voltage between the gate and the source (V_{GS}) so as to make constant the current between the source and the drain (I_{SD}).

3. Results and discussion

3.1. Reconstitution of PSI with molecular wires

The PSI of *Thermosynechococcus elongatus* BP-1 is composed of twelve protein subunits possessing a well-ordered electron-transfer chain. The molecular structure of PSI, the electron transfer mechanism and kinetics in PSI, and the treatment of living materials for the extraction of PSI have previously been investigated [17–22]. When PSI is irradiated, P700 is excited, and then a step-wise electron transfer from P700 to F_B via A_0, VK_1 (A_1), F_x, and F_A occurs without any backward transfer. These events induce a through-membrane charge separation, and the resulting efficiency of electron transfer is approximately 100% [7,8]. Here, *T. elongatus* was selected due to its high thermal stability at temperatures above 55 °C [23], and the efficient electron-transfer activity of the isolated PSI was assessed [24–26].

A schematic illustration of procedure for the reconstitution of PSI with molecular wire is shown in Fig. 2. Initially, VK_1 was extracted from the isolated intact PSI (Fig. 2a and b) using 50% water-saturated diethyl ether. Second, the VK_1-free PSI was reconstituted with a specifically designed molecular wire, $NQC_{15}S$-AuNP. This possesses three advantageous characteristics: (1) a naphthoquinone unit located at the end of a molecular wire to fit into the pocket where VK_1 had been extracted, (2) a redox potential of naphthoquinone suitable for the output of electrons from the A_0 site to a molecular wire, (3) a sufficient molecular length of the wire for the output of electrons from a pocket lacking VK_1 to a surface external to PSI. We employed an alkyl chain as the molecular wire. This is because the alkyl chain assists long-range transfer more effectively than space (the experimental decay constant of electron transfer rates, β, is ca. 1.0 for alkyl chains and 2.0–4.0 for space) [27]. The naphthoquinone-sulfur linked molecular wire equipped with a gold nanoparticle ($NQC_{15}S$-AuNP,

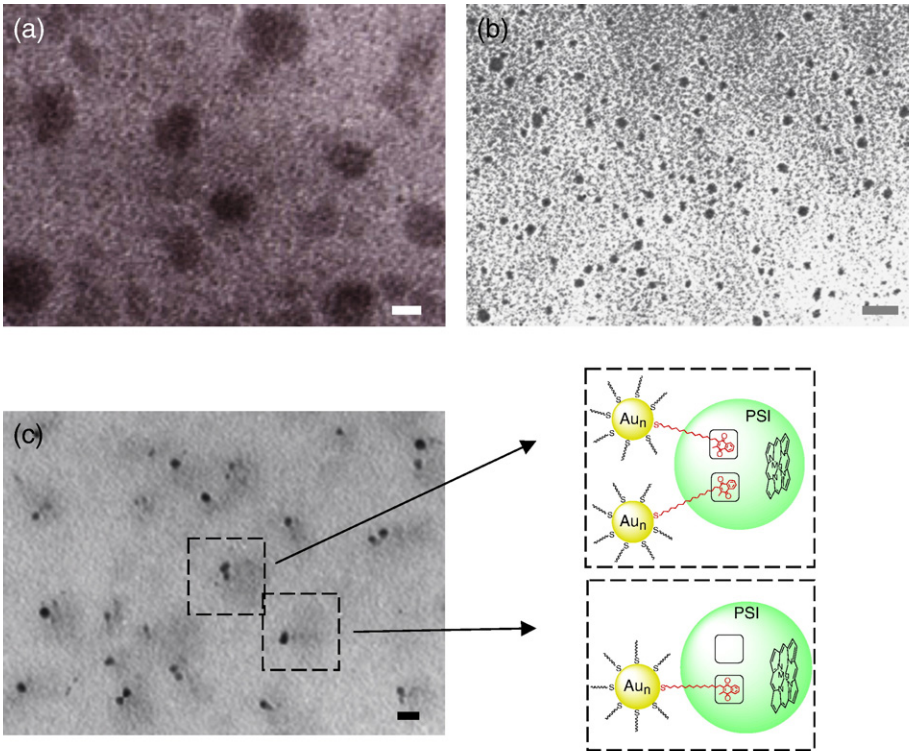

Fig. 4. TEM images of intact PSI (a), $NQC_{15}S$-AuNP (b), and $NQC_{15}S$-AuNP@PSI (c). The scale bar on each image is 10 nm.

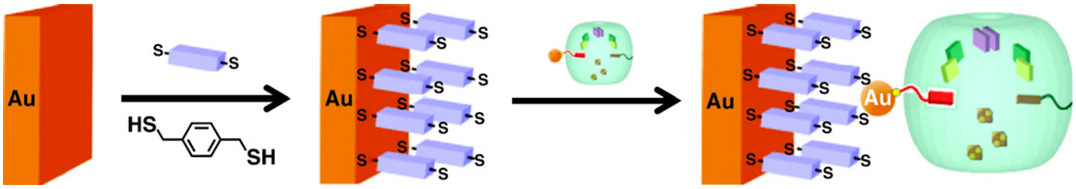

Fig. 5. Schematic illustration of the procedure for immobilization of NQC$_{15}$S-AuNP@PSI at a gold electrode.

particle size: ca 1.6 nm) [28] was treated with VK$_1$-free PSI in an MES-buffer solution under cool and dark conditions for 24 h to give NQC$_{15}$S-AuNP@PSI (Fig. 2c).

Actinic blue light irradiation to the intact PSI (7 μg chl mL^{-1}) induced absorption decrease at 701 nm by the formation of P700$^+$ (Fig. 3a). This phenomenon was brought by the higher speed of light induced electron efflux from PSI in comparison with the rate of electron influx from NaAs to P700$^+$. The VK$_1$-free PSI showed little absorption change because of quick backward electron transfer from A_0 to P700$^+$ (Fig. 3b). The reconstituted PSI with NQC$_{15}$S-AuNP again showed normal absorption decrease by blue light irradiation (Fig. 3c). This result indicated that the 2-methyl-1,4-naphthoquinone moiety of NQC$_{15}$S-AuNP fitted to the quinone pocket of PSI, and worked as a mediator of electron transport system in PSI.

Fig. 4 shows TEM images of intact PSI (a), NQC$_{15}$S-AuNP (b), and NQC$_{15}$S-AuNP@PSI (c). A TEM image of the intact PSI shown in Fig. 4a exhibited gray circles with diameters of ca. 20 nm and ca. 10 nm. These sizes could be assigned as a trimer (22 nm-o.d.) and a monomer (10 nm-o.d.) of PSI [15,29]. In the TEM image of NQC$_{15}$S-AuNP shown in Fig. 4b, black dots, of which diameter was 1.6±0.5 nm, were observed. In the image of NQC$_{15}$S-AuNP@PSI in Fig. 4c, both a large gray circle (10 nm-o.d.) and a small, clear, black dot (2 nm-o.d.) were observed, and every gray circle (PSI) has just 1 or 2 black dots (NQC$_{15}$S-AuNP). Because PSI has two VK$_1$ pockets, the stoichiometry of PSI and the gold nanoparticle(s) (i.e., 1 or 2) indicates that there were no random aggregations, and only connections via reconstitution at the VK$_1$ sites.

3.2. Immobilization of reconstituted PSI at a gold electrode and photocurrent measurement

In the next step, NQC$_{15}$S-AuNP@PSI was chemically connected to a gold electrode and photocurrent measurements of the modified electrode were carried out. Fig. 5 illustrates the procedures used for fabrication of the modified electrode. In order to connect the gold nanoparticle in NQC$_{15}$S-AuNP@PSI to a gold electrode, a SAM of 1,4-benzenedimethanethiol was prepared on the surface of the gold electrode. Then, NQC$_{15}$S-AuNP@PSI was immobilized on the SAM via Au-S bonding by immersing the SAM-modified gold electrode in a solution of reconstituted PSI. The amount of PSI immobilized on the gold electrode was estimated by QCM measurements to be 7.0×10^{-13} mol cm^{-2}, which is reasonable as monolayer coverage based on the size of PSI.

A photocurrent measurement of NQC$_{15}$S-AuNP@PSI-immobilized gold electrode was carried out in the presence of NaAs as a sacrificial reagent and DCIP as a mediator in a MES-NaOH (pH 6.4) buffer solution containing NaClO$_4$ as an electrolyte [30]. When the sample was irradiated with monochromatic light, photocurrent responses in the anodic direction were observed at 0 V vs. Ag/AgCl at all wavelengths; the action spectrum is shown in Fig. 6 (open circle). The action spectrum showed a clear peak at 680 nm, which is consistent with the absorption spectrum of PSI (dashed line). This result clearly indicated that these photocurrent responses were due to the photo-excitation of PSI.

3.3. Fabrication of an electronic imaging device: bio-photosensor

Practical application of this system as an electronic imaging device was examined by adapting the NQC$_{15}$S-AuNP@PSI to a gate of an FET (Fig. 7). The reconstituted PSI was immobilized on an Si_3N_4–Ta_2O_5 thin layer on the gate of an FET using silane coupling reaction and Au–S bond formation. The voltage–current characteristics of the NQC$_{15}$S-AuNP@PSI-modified FET under light irradiation at 670 nm (4 mW) are shown in Fig. 8. The light irradiation induced a marked change in the voltage between the gate and the source (V_{GS}) from −3.3 V to −5.4 V when the current between the drain and the source (I_{DS}) was below 1 μA. Light intensity affected the magnitude of V_{GS} (Fig. 9), thus indicating the potential use of this system in the interpretation of a grayscale image.

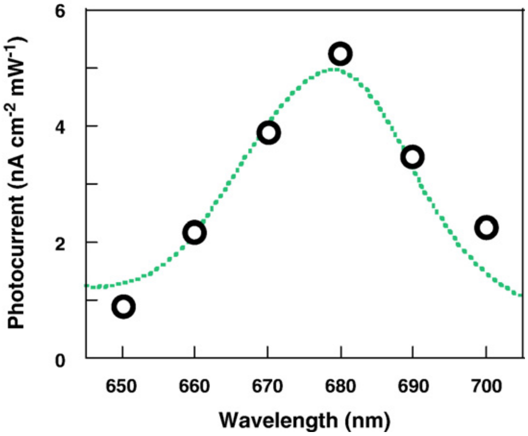

Fig. 6. A photocurrent action spectrum upon a NQC$_{15}$S-AuNP@PSI-immobilized gold electrode (○) in a MES-NaOH (pH 6.4) buffer solution containing 250 mM NaAs, 2.5 mM DCIP, and 100 mM NaClO$_4$ at E=0 V vs. Ag/AgCl. Dotted line is an absorption spectrum of 10 mg L^{-1} PSI MES-NaOH buffer solution.

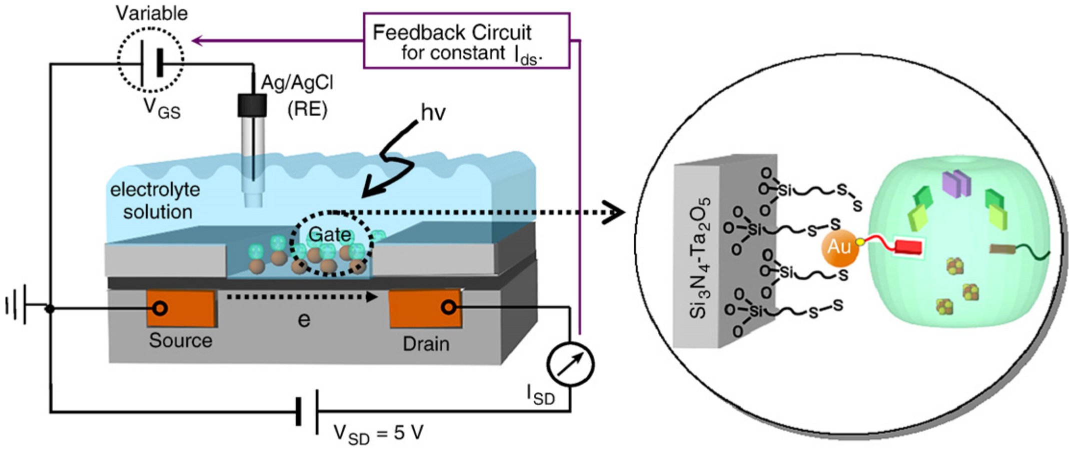

Fig. 7. Schematic illustration of the immobilization procedure of $NQC_{15}S$-AuNP@PSI on an FET.

Based on the results above, the image input experiment using the $NQC_{15}S$-AuNP@PSI-modified FET was carried out. Using the same experiment system as the above-mentioned photo response experiment, a computer and a projector were used instead of the light irradiation by LED, and then a grayscale picture of “Hokusai’s UKIYOE (Fugaku Sanju Rokkei-36 Views of Mt. Fuji)” divided into 60 × 80 pixels was projected to the gate part (Fig. 10a). The output signal (V_{GS}) in every pixel was detected by scrolling the image, and the image output was performed based on the acquired normalized value (Fig. 10b). The result demonstrates that the bio-photosensor made of cyanobacterial PSI coupled with transistor via molecular wire is practical. We repeated the same series of experiments at room temperature in intervals of several days, and this system was able to sustain its original level of performance for a period of more than 1 year.

Acknowledgements

This work was supported by Grants-in-Aid for Special Coordination Funds for Promoting Science and Technology Leading Research.

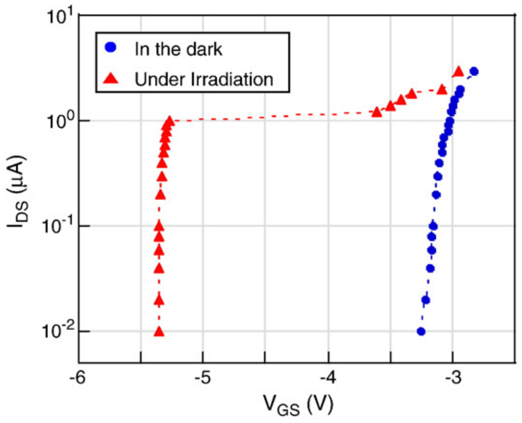

Fig. 8. Voltage–current characteristics of a $NQC_{15}S$-AuNP@PSI-immobilized FET with a logarithmic scale of I_{DS} in a MES-NaOH (pH 6.4) buffer solution containing 250 mM NaAs, 2.5 mM DCIP, and 100 mM $NaClO_4$. Under dark conditions (●) and light-irradiated conditions (670 nm, 4 mW) (▲).

Appendix A. Supplementary data

Supplementary data associated with this article can be found, in the online version, at doi:10.1016/j.bbabio.2006.11.008.

References

[1] K.M. Towe, On the origins of photosynthesis, Science 291 (2001) 436–437.

[2] J. Nelson, Solar cells by self-assembly? Science 293 (2001) 1059–1060.

[3] G.C. Dismukes, Splitting water, Science 292 (2001) 447–448.

[4] A.W. Rutherford, A. Boussac, Water photolysis in biology, Science 303 (2004) 1782–1784.

[5] H. Fukuzawa, E. Suzuki, Y. Komukai, S. Miyachi, A gene homologous to chloroplast carbonic Anhydrase (icfA) is essential to photosynthetic carbon dioxide fixation by synechococcus PCC7942, Proc. Natl. Acad. Sci. U. S. A. 89 (1992) 4437–4441.

[6] I.B. Frank, P. Lundgren, Y.B. Chen, H. Küpper, Z. Kolber, B. Bergman, P. Falkowski, Segregation of nitrogen fixation and oxygenic photosynthesis in the marine cyanobacterium trichodesmium, Science 294 (2001) 1534–1537.

[7] R. Emerson, R.V. Chalmers, C. Cederstand, Some factors influencing the long-wave limit of photosynthesis, Proc. Natl. Acad. Sci. U. S. A. 43 (1957) 133–143.

[8] R. Emerson, R.V. Chalmers, C. Cederstand, M. Brody, Effect of

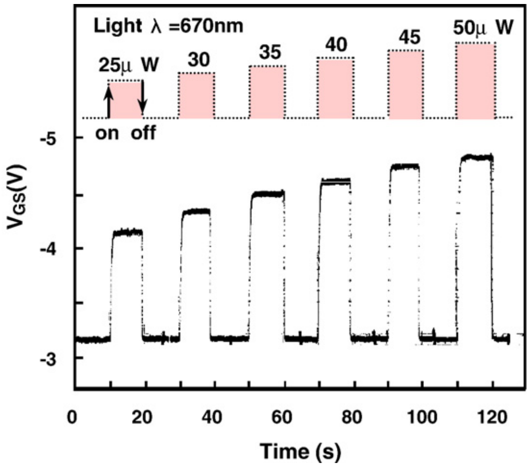

Fig. 9. Photo-response and light power dependency of V_{GS} for the $NQC_{15}S$-AuNP@PSI-immobilized FET.

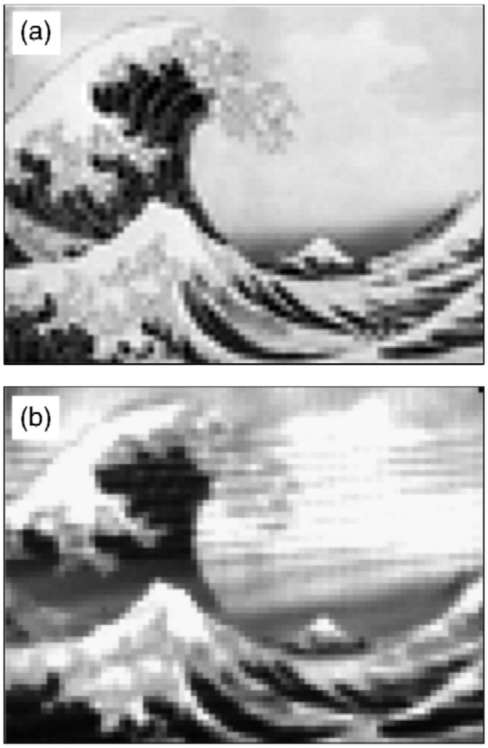

Fig. 10. An input image with 60 × 80 pixels (a) and the output image (b) obtained with the NQC$_{15}$S-AuNP@PSI-immobilized FET.

temperature on the long-wave limit of photosynthesis, Science 123 (1956) 673–674.

[9] As a success example, D. Gust, T.A. Moore, Mimicking Photosynthesis, Science 244 (1989) 35–41.

[10] A.F. Janzen, M. Seibert, Photoelectrochemical conversion using reaction-centre electrode, Nature 286 (1980) 584–585.

[11] R. Bhardwaj, R.L. Pan, E.L. Gross, Solar conversion by chloroplast photoelectrochemical cells, Nature 289 (1981) 396–398.

[12] I. Lee, J.W. Lee, E. Greenbaum, Biomolecular electronics: vectorial arrays of photosynthetic reaction centers, Phys. Rev. Lett. 72 (1997) 3294–3297.

[13] E. Katz, Application of bifunctional reagents for immobilization of proteins on a carbon electrode surface: oriented immobilization of photosynthetic reaction centers, J. Electroanal. Chem. 365 (1994) 157–164.

[14] B.S. Ko, B. Babcock, G.K. Jennings, S.G. Tilden, R.R. Peterson, D. Cliffel, E. Greenbaum, Effect of surface composition on the adsorption of photosystem I onto alkanethiolate self assembled monolayers on gold, Langmuir 20 (2004) 4033–4038.

[15] S.O. Wenk, J. Kruip, Rapid purification of the membrane protein photosystem I by high performance liquid chromatography on porous materials, J. Chromatogr., B 737 (2000) 131–142.

[16] E.E. Foos, A.W. Snow, M.E. Twigg, M.G. Ancona, Thiol terminated Di, Tri, and tetraethylene oxide functionalized gold nanoparticles: a water soluble, charge neutral cluster, Chem. Mater. 14 (2002) 2401–2408.

[17] P. Jordan, P. Fromme, H.T. Witt, O. Klukas, W. Saenger, N. Krauβ, Three dimensional structure of cyanobacterial photosystem I at 2.5 Å resolution, Nature 411 (2001) 909–917.

[18] P. Fromme, P. Jordan, N. Krauβ, Structure of photosystem I, Biochim. Biophys. Acta 1507 (2001) 5–31.

[19] K. Brettel, Electron transfer and arrangement of the redox cofactors in photosystem I, Biochim. Biophys. Acta 1318 (1997) 322–373.

[20] S. Bahatyrova, R.N. Frese, C.A. Siebert, J.D. Olsen, K.O. van der Werf, R. van Grondelle, R.A. Niederman, P.A. Bullough, C. Otto, C.N. Hunter, The native architecture of a photosynthetic membrane, Nature 430 (2004) 1058–1062.

[21] A. Ben Shem, F. Frolow, N. Nelson, Crystal structure of plant photosystem I, Nature 426 (2003) 630–635.

[22] C.W. Mullineaux, M.J. Tobin, G.R. Jones, Mobility of photosynthetic complexes in thylakoid membranes, Nature 390 (1997) 421–424.

[23] T. Yamaoka, K. Satoh, S. Satoh, Photosynthetic activities of a thermophilic blue green alga, Plant Cell Physiol. 19 (1978) 943–954.

[24] H. Koike, K. Satoh, S. Katoh, Heat stabilities of electron transport related to photosystem I in a thermophilic blue green alga, Synechococcus sp, Plant Cell Physiol. 23 (1982) 293–299.

[25] B.L. Epel, J. Neumann, The mechanism of the oxidation of ascorbate and Mn^{2+} by chloroplasts, Biochim. Biophyd. Acta 325 (1973) 520–529.

[26] M. Iwaki, S. Ito, Electron transfer in spinach photosystem I reaction center containing benzo, naphtho- and anthraquinones in place of phylloquinone, FEBS Lett. 256 (1989) 11–16.

[27] H.B. Gray, J.R. Winkler, Long-range electron transfer, Proc. Natl. Acad. Sci. U. S. A. 102 (2005) 3534–3539.

[28] S. Chen, R.S. Ingram, M.J. Hostetler, J.J. Pietron, R.W. Murray, T.G. Schaaff, J.T. Khoury, M.M. Alvarez, R.L. Whetten, Gold nanoelectrodes of varied size: transition to molecule-like charging, Science 280 (1998) 2098–2101.

[29] T.S. Bibby, J. Nield, J. Barber, Iron deficiency induces the formation of an antenna ring around trimeric photosystem I in cyanobacteria, Nature 412 (2001) 343–345.

[30] N. Terasaki, N. Yamamoto, H. Takashi, I. Sato, S. Y. Inoue, Fabrication of novel photosystem I-gold nanoparticle hybrids and their photocurrent enhancement, Thin Solid Films 499 (2006) 153–157.